An insight of enhanced natural material (calcined diatomite) efficiency in nickel and silver retention: Application to natural effluents

Youssef El Ouardi, Catherine Branger, Hamid Toufik, Katri Laatikainen, Abdelkrim Ouammou, Véronique Lenoble

Version of Record: https://www.sciencedirect.com/science/article/pii/S2352186419306297
Manuscript_2cd3d6e5cc7ffb421449e1e795eeb952

An insight of enhanced natural material (calcined diatomite) efficiency in nickel and silver retention: application to natural effluents.

Youssef El Ouardi[1-2-3], Catherine Branger[2], Hamid Toufik[4], Katri Laatikainen[5], Abdelkrim Ouammou[3], Véronique Lenoble[1*]

[1] *Université de Toulon, Aix Marseille Univ, CNRS, IRD, MIO, France*

[2] *Université de Toulon, MAPIEM, Toulon, France*

[3] *Université Sidi Mohamed Ben Abdellah, Faculté des Sciences Dhar El Mehraz, LIMOM Laboratory, Dhar El Mehraz B.P. 1796 Atlas, Fès 30000, Morocco*

[4] *University Sidi Mohamed Ben Abdellah- Fès, LMSNEM Laboratory, Faculté Polydisciplinaire de Taza, Maroc*

[5] *Lappeenranta-Lahti University of Technology, Laboratory of Computational and Process Engineering, P.O. Box 20, FI-53851 Lappeenranta, Finland*

* Corresponding author: lenoble@univ-tln.fr (V. Lenoble).

Abstract

Natural diatomite is widely used worldwide as an alternative to synthetic adsorbents and its adsorbing capacity towards nickel and silver ions is assessed in this work. Diatomite was heated up to 550, 750 or 950 °C to modify its physico-chemical and binding properties. A thorough characterization of the resulting material was done by X-ray diffraction, Fourier Transform Infrared Spectroscopy (FTIR), ThermoGravimetric Analysis (TGA), Scanning Electron Microscopy (SEM) and porosity measurements. The adsorption of nickel and silver ions onto these materials was studied as a function of the adsorbent concentration, organic matter as well as the presence of competitor ions. Diatomites demonstrated a better retention capacity when compared to materials of close composition. Best removal capability was obtained by calcination at 550 °C. This

material was successfully tested for nickel and silver removal from both natural river waters as well as industrial wastewater. Due to high regeneration and reusability, this low cost, easily prepared, natural material may be an attractive alternative for adsorbent in wastewaters treatment.

Keywords: diatomite, nickel, silver, adsorption, isotherm, effluents

1. Introduction

Trace metals have been and are still extensively used for industrial (metal plating facilities, mining operations) and agricultural (pesticides) purposes (Fu and Wang, 2011). They are ubiquitous in the environment and represent a long-term danger by accumulating in bones and organs over time (Nriagu, 1988). Nickel is one of the most dangerous pollutants, extremely toxic (Cempel and Nikel, 2006) as it is responsible for different types of cancer (Dey et al., 2018). Silver is currently attracting attention for its valuable antibacterial properties, at a time when antimicrobial resistance has now become a real public health problem (Gunasekaran et al., 2012). Its use is therefore more and more common and extended, despite its demonstrated toxicity (Marimuthu et al., 2020; Nam and An, 2019). Nickel and silver are worryingly present in the industrial effluents of a majority of countries (Susan E, 1999).

The brassware industry, a famous industrial activity in Fez area (one of the most touristic area in Morocco), produces effluents heavily contaminated by nickel and silver. These effluents are not subjected to any treatment and are directly discharged into the environment. Not only these inputs are a significant risk for the environment, they are also one of the main problems for the wastewater treatment plant in Fez city (Hayzoun et al., 2015) as nickel and silver can reach up to 215 and 95 $\mu g.L^{-1}$, respectively (see Table 1) .

The removal of toxic metals from wastewater is an active area of research. The most used technologies include adsorption, precipitation, ion exchange, coagulation, evaporation and reverse osmosis (Uddin, 2017). Among these different techniques, the adsorption process is one of the most popular due to its rather simple application and in some cases, very effective removal. Various natural adsorbents have been used: kaolinite, activated charcoal, natural and synthetic zeolites or clays (Belkhiri et al., 2012; Gu et al., 2018; Wu et al., 2009). The adsorbent cost is a key point for their commercial and industrial use (Liu et al., 2019) as well as their overall stability, adsorbing capacity as well as ubiquity.

Diatomites are rocks formed by the accumulation of unicellular algae frustules (Bahramian et al., 2010). Their composition predominantly includes 60 to 75 % SiO_2, 2 to 4 % Fe_2O_3 and 5 to 8 % of CaO. They are used in many fields: filtration and purification by active principle, clarification of liquid food, construction (Liang et al., 2015), and even as an alternative towards the use of chemical pesticides (Doumbia et al., 2014). After a specific treatment (e.g. drying, grinding or calcination), diatomite can be made in a powder of very high porosity having important adsorption and filtration properties (Chang et al., 2020). This material is fairly abundant and easily accessible in Fez area.

This study is focusing on the adsorbing capacity of diatomite towards nickel and silver ions, either as a raw material (raw-Da) or after thermal treatment at different temperatures: 550, 750 and 950 °C (Da550, Da750 and Da950 respectively). We first studied the adsorbing capacity of all these materials towards nickel. We showed that Da550 gave the most promising results and we then used this material for the simultaneous removal of nickel and silver, the two main contaminants of Fez City

brassware effluents, and assessed their mutual influence/competition. Da550 was also tested in natural river waters and in brassware effluent. These results represent an initial stage to promote the use of natural, cheap and abundant diatomite as an efficient adsorbent for contaminants threatening Morocco's most touristic area.

2. Materials and Methods

2.1. Solids preparation

The diatomite was collected in the Tighza deposit, situated in the northeastern region of Morocco. The raw diatomite was sieved and the fraction below 100 μm was collected. This material was separated in different portions, which were subsequently calcined under air atmosphere at three different final temperatures: 550, 750 and 950 °C, in a programmable furnace applying a heating rate of 5 °C/min, from room temperature to the selected calcination temperature and with constant cooling rate of 5 °C/min. The samples were left in the furnace for 6h at the calcination temperature.

2.2. Solids characterization

The pH of the dispersions formed by the diatomite (as raw and calcined materials) was directly measured on a sample of 0.1 g dispersed in 10 mL of deionized water.

The total carbon analysis in samples was obtained with a Thermal Scientific Flash 2000 NC Soil Analyzer. A mass of 12 mg of sample was placed in a tin capsule. Carbon was measured by flash combustion at 930 °C (Hayzoun et al., 2014). The limit of detection was 5 μg C and the calibration curve ranges from 10 to 1100 μg C.

Powder X-ray diffraction (XRD) patterns of the samples were obtained with a X'Pert Pro panalytical diffractometer using a Cu Kα radiation at 40 kV and 30 mA with a scan range of 5–2θ–70°, a scan speed of 0.02°2θ per 2s, and a step size of 0.02° 2θ.

The Fourier-Transform infrared (FTIR) spectra were obtained on a Bruker Vertex70 spectrometer. About 1 mg of sample was mixed with approximately 300 mg of dried KBr and pressed to form pellets. The measurements were carried out over the range 4000–400 cm^{-1} in the transmittance mode, with a spectral resolution of 4 cm^{-1}.

Themogravimetric analysis (TGA) was obtained on a SDT-TGA Q600. Samples (approximately 10 mg) were inserted in ceramic pans submitted to heating (10 °C/min heating rate) from 30 to 1000 °C in a flowing air atmosphere of 100 mL/min.

For scanning electron microscopy (SEM) and energy dispersive X-ray spectroscopy (EDX), samples were metalized by a thin gold layer and SEM images were taken using a Supra 40 VP microscope (Gemini). This equipment has an Oxford 7060 X-ray spectroscopy system through dispersive energy (EDX), which enables qualitative evaluation of the chemical composition.

The specific surface areas were determined according to the Brunauer Emmet–Teller (BET) equation with nitrogen adsorption–desorption isotherms at 77K using a Micrometrics Gemini V apparatus.

2.3. Reagents

High purity deionized water (conductivity 0.05 µS/cm at 25 °C, Milli-Q system) was used to prepare all the solutions in the various experiments. Nickel (II) nitrate hexahydrate (99.9 %, $Ni(NO_3)_2.6H_2O$) was used as received from Sigma Aldrich. Ag(I) Silver nitrate (≥ 99.7 %, $AgNO_3$) was purchased from Fisher Scientific (Analytical Grade). N-(2-Hydroxyethyl)piperazine-N-2-ethanesulfonic Acid (≥ 99 %, HEPES) from Fisher Scientific was used to buffer the solutions.

The dissolved organic matter used was Humic Acid from Sigma Aldrich (Technical grade). For all experiments, vessels (Corning® tubes, syringes, filters, etc.) were pre-

cleaned before use with HNO_3 washing (10 %, Fisher, Analytical Grade) then thoroughly rinsed with milliQ water.

2.4. Adsorption experiments

The adsorption experiments were carried out at room temperature in 50 mL Corning© tubes by mixing a fixed amount of adsorbent (0.4 g) with 40 mL of aqueous solution. Aqueous solutions were prepared by dissolving $Ni(NO_3)_2 \cdot 6H_2O$ and $AgNO_3$, respectively, in milliQ water to reach the desired concentrations. The mixtures were shaken with an orbital shaker at a speed of 80 rpm during 180 min. For all experiments except that with natural effluents, the pH of the dispersions was adjusted to 7.0 using HEPES buffer. No pH influence study was performed as the final aim of our work is the application to natural effluents. All experiments were carried out in duplicate. At the end of the adsorption experiments, dispersions were centrifuged at 5000 rpm for 5 min. The supernatant was then filtered with Syringe Filters, 0.45 µm - Surfactant - Free Cellulose Acetate. The filtrates were acidified with suprapur® HNO_3 at pH < 2 and stored at 4°C until their analysis.

The influence of the amount of Da550 adsorbent on nickel and silver retention was examined (0.4 g; 0.8 g; 1.2 g; 1.6 g; 2 g and 3 g/40 mL). The initial nickel or silver concentration was 65 mg/L, in the range of concentrations encountered in brassware effluents (Table 1).

Nickel retention was studied on all materials (raw and calcined diatomite) over a wide concentration range, from 10 to 130 mg/L in buffered milliQ water, in order to better model the adsorption mechanisms. Silver retention was studied on Da550 only, as it was the material giving the best retention results towards Ni. The studied concentration range was 10 to 130 mg/L. These values were chosen to frame the real contaminant

levels in the most contaminated effluent considered in this study (80.3 and 41.7 mg/L, for nickel and silver respectively).

In order to assess the effect of the organic matter on nickel retention, experiments were carried out with two concentrations of dissolved organic matter (30 and 60 mg/L) and two concentrations of nickel (50 and 120 mg/L).

Nickel and silver competition on Da550 were studied in binary-component system. The experiments were carried out a ratio of 1:1 Ni:Ag, with nickel and silver concentrations equally ranging between 10 to 130 mg/L.

Nickel and silver retentions on Da550 were studied in various effluents: effluents from the brassware industry (A) and effluents from Sebou (S1, S2) and Fez (F1, F2) rivers. Effluents from the brassware industry was directly collected from the rinsing baths before discharge in Fez river. The effluents from Fez and Sebou rivers were collected downstream from Fez city and downstream from the confluence with the river Fez respectively, either during a period of brassware fabrication (F1 and S1) or during a non-working day (F2 and S2). The composition of each effluent is given in Table 1.

Table 1. Trace element concentrations and dissolved organic matter (DOC) in the brassware effluents (A), Fez (F) and Sebou (S) rivers. F1 and S1 were sampled during a period of brassware fabrication. F2 and S2 were sampled during a non-working day.

	Ni (µg/L)	**RSD %**	**Ag (µg/L)**	**RSD %**	**DOC (mg/L)**	**SD (mg/L)**
A	80300	1.3	41700	0.31	80.7	0.18
F1	214.6	7.2	94.3	1.8	28.8	0.4
F2	59.5	1.4	51.1	1	19.4	0.2
S1	122.8	1.4	28.9	2.4	9.2	0.14

S2	20.4	2.6	5.1	1.1	7.3	0.04
EQS	20	-	5	-	-	-

EQS: Environmental Quality Standard.
RSD: Relative Standard Deviation.

In order to examine the reusability of the adsorbent, the used material was agitated with 10 mL of 0.05 mol/L HNO_3 for 30 min, washed three times with milliQ water to remove the excess of trace metals and acidity and finally dried at 60 °C for 24h. Then, nickel and silver adsorptions were repeated in the same conditions as before. The regeneration cycle was repeated five times. For all experiments, trace metal concentrations were measured using ICP-OES (Perkin Elmer - Optima 7300 DV).

2.5. Isotherms and adsorption models

Equilibrium isotherms for nickel and silver were obtained by performing batch adsorption studies. The amount of the metal ion adsorbed per unit mass of the adsorbent at equilibrium, q_e (mg/g), and the adsorption rate (%) were calculated from the expressions:

$$q_e = \frac{(C_0 - C_e)}{m} \times V \qquad (1)$$

$$\% \text{ Adsorption} = \frac{(C_0 - C_e)}{C_0} \times 100 \qquad (2)$$

where C_0 (mg/L) is the metal ion initial concentration in the solution, C_e (mg/L) is the metal ion concentration at equilibrium in the dissolved phase, m is the mass of adsorbent (g) and V is the volume of solution (L).

The adsorption data were analyzed using Langmuir (Langmuir, 1918) and Freundlich (Freundlich, 1906) models. Langmuir model is based on a homogeneous surface with a

finite number of identical sites, assuming no interaction between adjacent sites. It is expressed as:

$$\frac{C_e}{q_e} = \frac{1}{K_L q_m} + \frac{C_e}{q_m} \qquad (3)$$

where q_m (mg/g) refers to the maximum adsorption capacity and K_L (L/mg) is the Langmuir constant.

The Freundlich model supposes that adsorption occurs onto a heterogeneous surface. This model is expressed by the following equation:

$$q_e = K_F C_e^{1/n} \qquad (4)$$

Freundlich linearization follows:

$$\mathrm{Ln}\ q_e = \mathrm{Ln}\ K_F + \frac{1}{n}\ \mathrm{Ln}\ C_e \qquad (5)$$

where K_F and n are Freundlich constants related to the adsorption capacity and the strength of adsorption respectively.

Another parameter was considered: the rate of equilibrium adsorption reduction (Δ) (Zhi-rong and Shao-qi, 2009). It is the ratio of the difference between non-competitive equilibrium adsorption and competitive equilibrium adsorption to non-competitive adsorption observed at equilibrium:

$$(\Delta)\% = \frac{(q_i m - q_i mix)}{q_i m} \times 100 \qquad (6)$$

where $q_i m$ (mg/g) and $q_i mix$ (mg/g) are the maximum adsorption capacity of i species in the single component system and binary component system, respectively.

3. Results and discussion

3.1. Physico-chemical characterization of raw and modified diatomites

All raw samples presented a low organic content (<1.2 %) (Table 2). After heating treatment above 550 °C, total carbon became negligible in accordance with the total calcination of the organic matter. The pH values of aqueous solutions of the diatomite samples (raw-Da, Da550, Da750, Da950) were measured to be 9.6, 10.9, 11.1 and 10.5, respectively. This indicates that diatomite thermal treatment gives a more basic character to its aqueous solutions, probably due to the fact that diatomite acidic sites are weak, and their strength further decrease when the thermal treatment is applied, leading to less proton being released.

Table 2. Physico-chemical properties of diatomite samples (N: number of analyzed samples, nd: not detected).

N=3	**raw-Da**	**Da550**	**Da750**	**Da950**
Total carbon (%)	1.15±0.02	0.8±0.03	≤0.01	nd
pH	9.6±0.15	10.9±0.1	11.1±0.03	10. 5±0.1
S_{BET} (m^2/g)	11.13±0.14	10.32±0.25	7.9±0.3	5.53±0.3
Porous volume (cm^3/g)	0.02	0.02	0.016	0.008

XRD patterns of the raw and calcined diatomite are shown in Figure 1. Table 3 summarizes the Bragg angles (2θ) of the studied diatomites phases. The main peaks in the raw diatomite sample correspond to quartz (characterized by Bragg angles 2θ =20.9°, 26.7°, 36.4°, 50.2° and 59.9°) and calcite (2θ =29.5°). The XRD patterns of the raw sample were different from the calcined ones, where the amounts of magnetite (Fe_3O_4) and feldspar $Na(AlSi_3O_8)$ increased with the calcination temperature, as seen by the angles of incidence (2θ =27.8° and 30.04°). Thermal treatment at the highest temperatures seemed to lead to a complete structural modification. This behavior is in agreement with earlier reports on thermal treatment (Arik, 2003; Inchaurrondo et al., 2016).

Table 3. Bragg angles of the studied diatomites phases.

System	quartz	calcite	feldspar	magnetite
raw-Da	2θ = 20.9, 26.7, 36.4, 39.4, 50.2 and 59.9	2θ = 29.5	_	_
Da550	2θ = 20.9, 26.7, 36.4, 39.4, 50.2 and 59.9	2θ = 29.5	_	_
Da750	2θ = 20.9, 26.7, 36.4, 39.4, 50.2 and 59.9	2θ = 29.5	_	_
Da950	2θ = 20.9, 26.7, 36.4, 39.4, 50.2 and 59.9	_	2θ = 27.8	2θ = 30.04

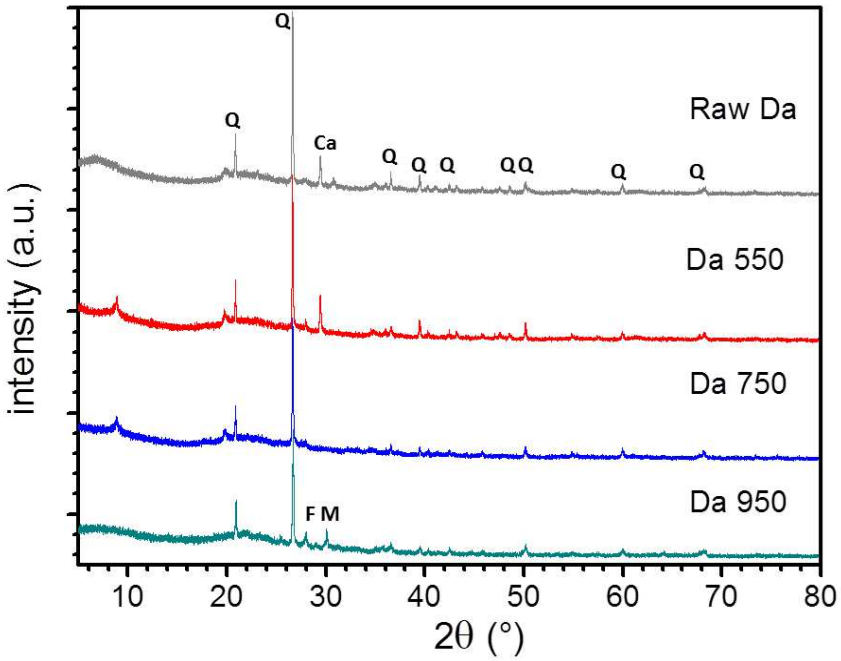

Figure 1. Powder XRD profiles of raw-Da, Da550, Da750 and Da950. (Q: quartz, Ca: calcite, F: feldspar, M: magnetite).

The FTIR spectra of the raw and calcined diatomites are presented in Figure 2. The raw diatomite presented distinctive bands at 3625, 1633, 1433, 1043, 795 and 448 cm^{-1}. The band at 3625 cm^{-1} was due to the free silanol group (SiO-H) (Khraisheh et al., 2005;

Mohamedbakr and Burkitbaev, 2009), the band at 1633 cm^{-1} to the flexural vibration H-O-H of water, while the band located around 1433 cm^{-1} could be attributed to the carbonate issued from the calcite fraction of the diatomite. The band at 1043 cm^{-1} corresponded to Si-O-Si stretching (Chaisena and Rangsriwatananon, 2004; Inchaurrondo et al., 2016; Mohamedbakr and Burkitbaev, 2009). The band at 795 cm^{-1}, related to the free silica, was found in all diatomite materials (inter tetrahedral Si-O-Si bending). The absorption peak around 448 cm^{-1} corresponded to the Si-O-Si bending vibration (Mohamedbakr and Burkitbaev, 2009). After thermal treatment at different temperatures, the absorption peak corresponding to the OH groups at 3625 cm^{-1} as well as the peaks at 1633 cm^{-1} and 1433 cm^{-1}, related to the presence of adsorbed water and the carbonate, respectively, disappeared. On the contrary, the bands at 1043 cm^{-1} and 795 cm^{-1} were not affected by the thermal treatment. FTIR analyzes thus confirm the impact of thermal treatments on diatomite structures, as also shown by the XRD study. Such modifications will likely have an impact on their adsorption properties.

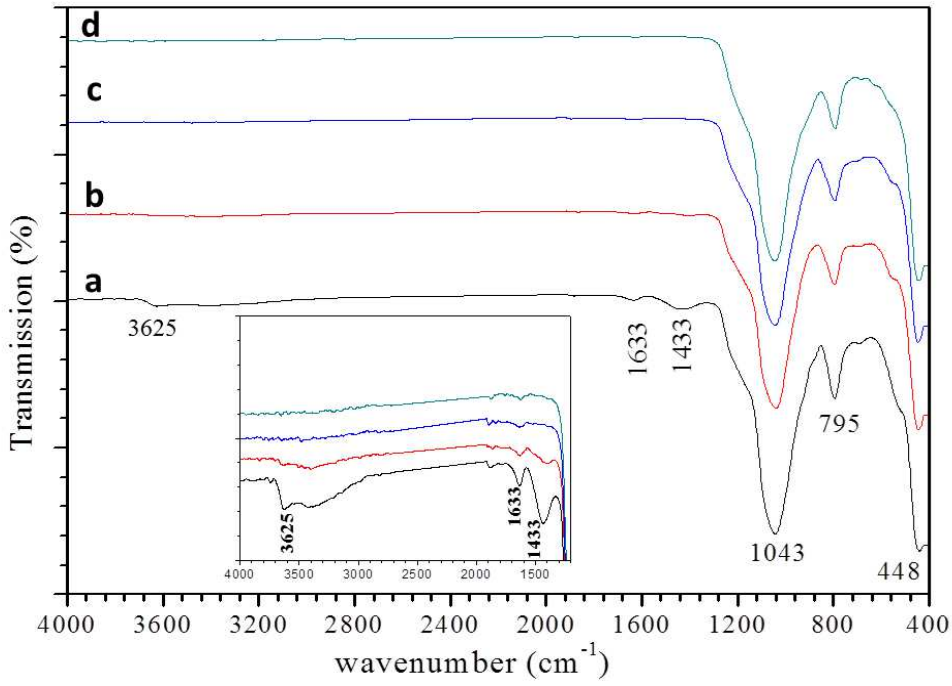

Figure 2. FTIR spectra of raw-Da (a), Da550 (b), Da750 (c) and Da950 (d)

The thermogravimetric curves of the raw and calcined diatomite samples are shown in Figure 3. There was a total weight loss of 11.2 %, 6.4 %, 2.01 % and 1.87 % for raw diatomite, Da550, Da750 and Da950 respectively. For Da750 and Da950, the structure seemed altered by the thermal treatment, as no further variation could be seen. Such alteration was also visible with XRD and FTIR results, which also proved that these two materials were completely different from the raw diatomite. As a result, these samples materials will probably present low adsorption capacities. For raw diatomite and Da550, TGA curves showed a weight loss at temperatures below 200°C, due to the removal of the adsorbed water (Chaisena and Rangsriwatananon, 2004; Zhou et al., 2016). This loss is more pronounced for raw-Da as this material contains more water (as demonstrated by FTIR). Above 200 °C, the observed important weight loss for raw-Da must be due to the dissociation of the coordinated water and the condensation reactions occurring between the Si-OH groups of the silanol (Zhou et al., 2016). The observed mass losses above 600 °C were in agreement with the total carbon content as, at 950 °C, there is the complete removal of organic matter.

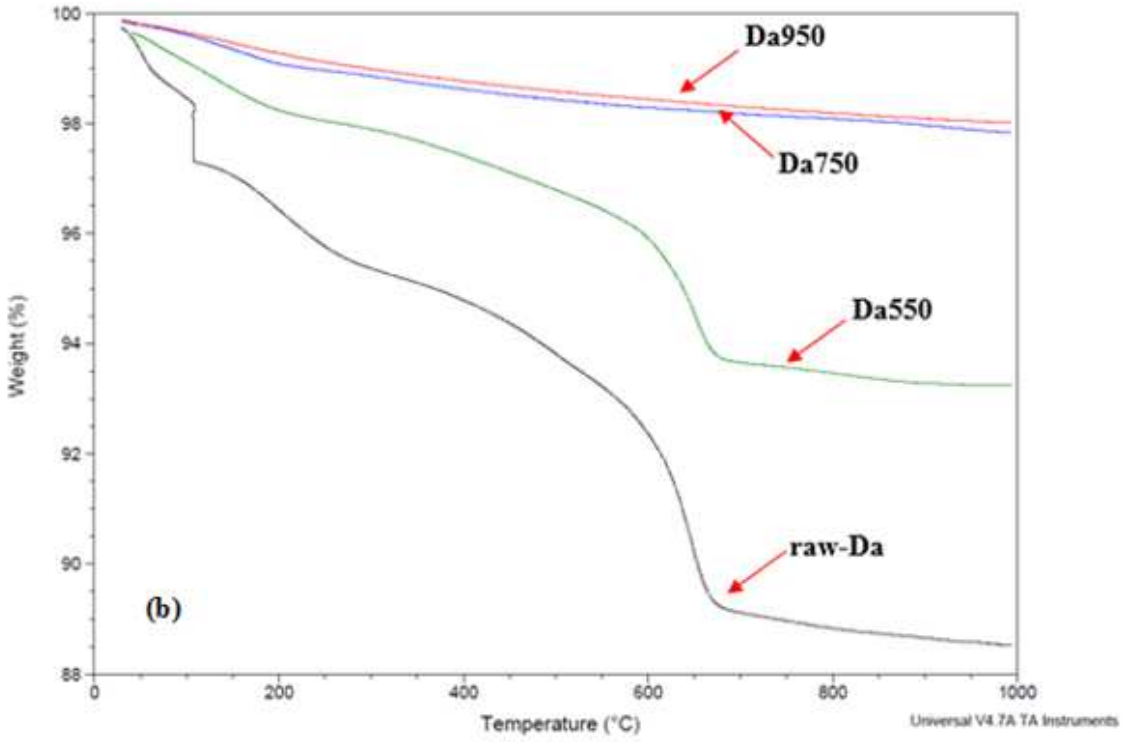

Figure 3. TGA profile of raw-Da, Da550, Da750 and Da950.

3.2. Morphological characterization of the raw and modified diatomites

SEM images of the raw and calcined diatomite are shown in Figure 4. The heterogeneous structure of diatomite can clearly be seen along with the different shapes of diatoms frustules. Such frustules are divided into two main categories: centric diatoms with radial symmetry and pennate diatoms with axial symmetry (Al-Degs et al., 2001). The morphology of raw-Da fluctuates as a function of the calcination temperature (Figs. 4b to 4d) with a significant decrease of the pore diameter: 1.5-3.1 µm for raw diatomite (Fig. 4e) but down to 335-850 nm for calcined samples (Fig. 4f).

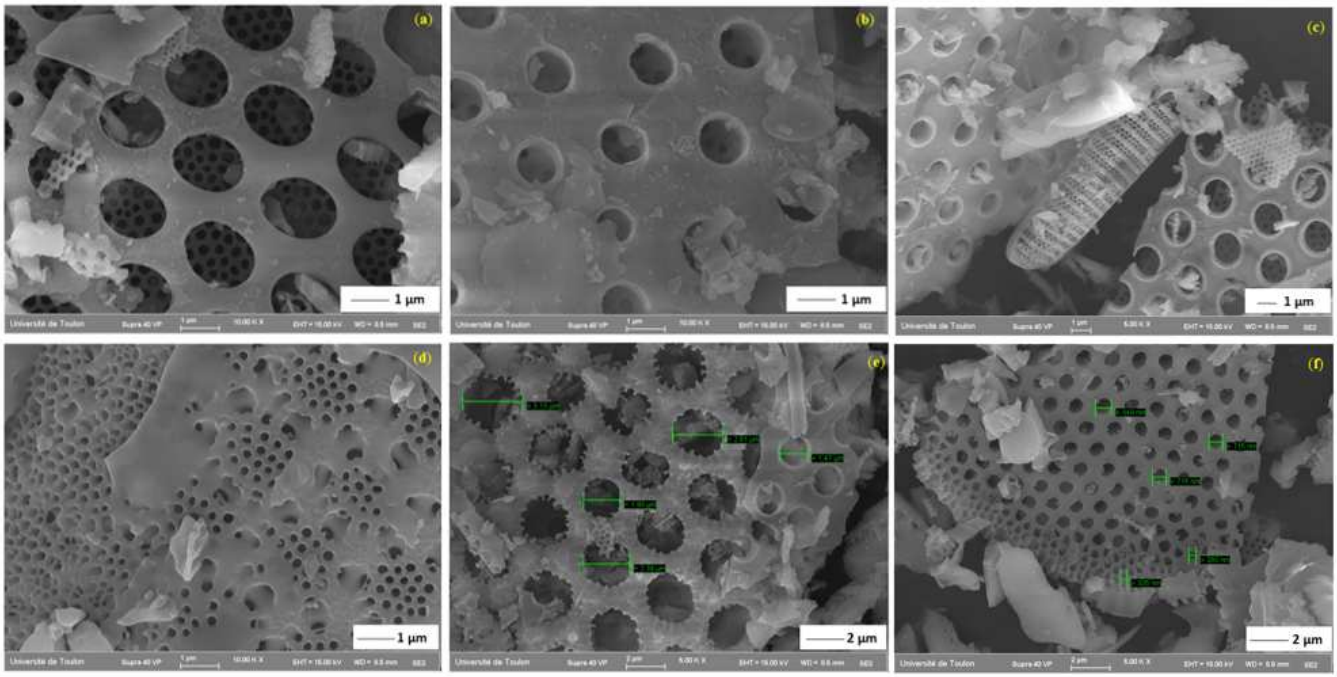

Figure 4. SEM images of raw-Da (a), Da550 (b), Da750 (c) and Da950 (d), pores in the diatom frustule of raw-Da (e) and pores in the calcined diatom Da950 (f).

The nitrogen adsorption/desorption experiments are presented in Fig.5. From the shape of the obtained isotherms, it was concluded that the studied diatomites were macroporous according to the International Union Of Pure And Applied Chemistry – IUPAC nomenclature (Stafford et al., 1985; Thommes et al., 2015). These results were in accordance with the SEM observations. From these experiments, the specific surface area (BET) and the total pore volume of raw-Da were evaluated to 11.1 m^2/g and 0.02 cm^3/g, respectively (Table 2). When considering Da550, Da750 and Da950, a continuous decrease was observed in the BET surface area and pore volume when the temperature increases, in accordance with previous observations and the demonstration of structural damage. This can be explained by a welding together of the diatomite particles upon temperature increase, finally leading to a sintering of the material. This modification is especially noticeable for the higher thermal treatment. This process

leads to the observed decrease in the pore volume and size as well as the specific surface area.

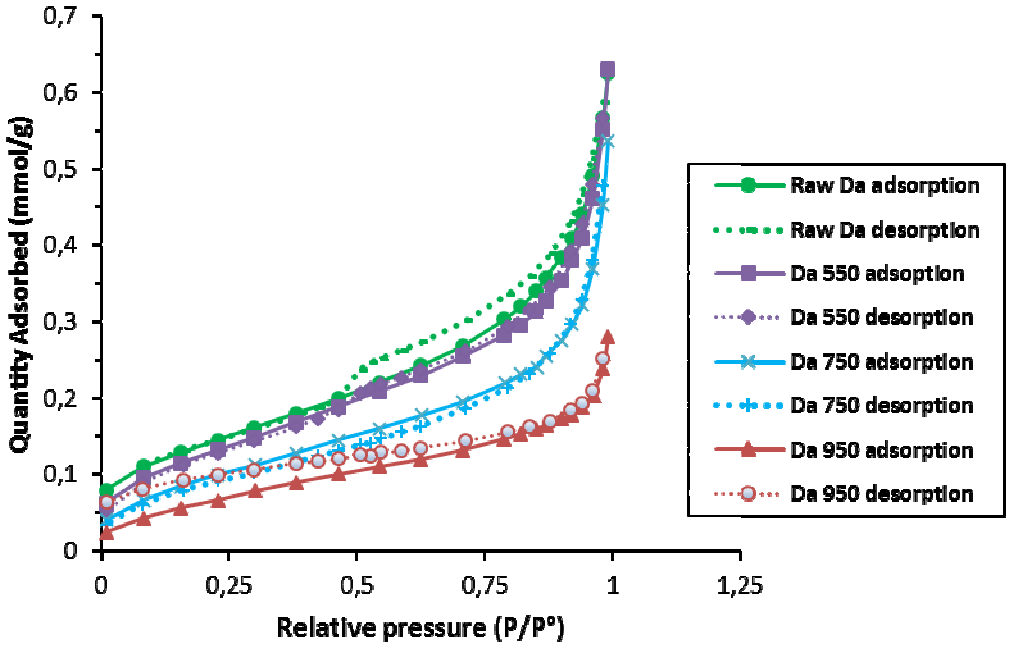

Figure 5. Nitrogen adsorption and desorption isotherms at 77K of diatomite samples

3.3. Nickel and silver retention in single-component systems

A preliminary study was achieved to define the optimum liquid /solid ratio to be used for the metal adsorption experiments, using Da550 as the adsorbent. The results showed a significant decrease in the amount of both adsorbed nickel and silver with the amount of Da550 (Fig. 6). This may be due to particle aggregation at higher adsorbent mass (Sen and Bhattacharyya, 2008; Vieira et al., 2010) resulting in an overall decrease of the surface area. For the following experiments, an amount of 0.4 g of solid phase was systematically used (liquid/solid ratio of 1/10).

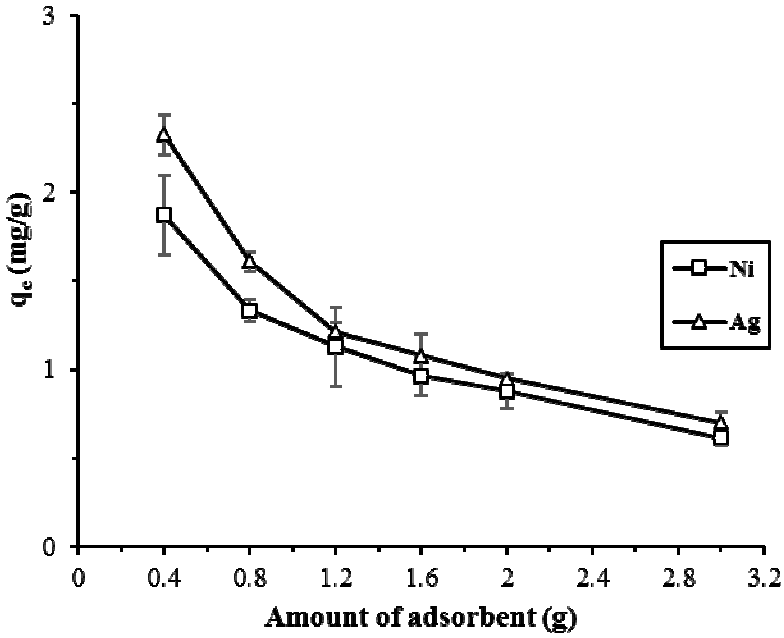

Figure 6. Effect of Da550 amount on the adsorption of nickel and silver (initial concentration of 65 mg/L; V = 40mL).

The equilibrium isotherms demonstrated the effect of diatomite thermal treatment on nickel adsorption (Fig. 7): the retention capacity increased from raw-Da to Da550 (1.9 to 2.9 mg/g), then constantly decreased down to 1.3 mg/g. Such decrease was due to the very low specific surface area and the thermal inherent sintering process. The structural alteration of Da750 and Da950 therefore led to lower adsorption capacity, in general agreement with the characterization results.

Langmuir (Eq (3)) and Freundlich models (Eq (5)) were both used to fit the adsorption isotherms. The corresponding Freundlich and Langmuir parameters along with correlation coefficients are given in Table 4. The correlation coefficients showed that Freundlich model better fitted the results for all the diatomite samples. The values of n (all higher than 1) reflect the favorable adsorption of nickel and silver ions onto the adsorbent surface (El-Sadaawy and Abdelwahab, 2014). This indicates that the

diatomite surface is heterogeneous, which suggests that nickel and silver ions adsorption rather follows multilayer adsorption. The n values indicate the degree of nonlinearity between solution concentration and adsorption as follows: if n = 1, the adsorption is linear; if n < 1, the adsorption is a chemical process; if n > 1, then adsorption is a physical process (Farhan et al., 2013). The n values were found higher than 1, suggesting that the adsorption of nickel and silver ions on diatomite samples occurs physical adsorption (e.g. Van der Waals forces). Such modeling fitting is in agreement with the heterogenous structure demonstrated through the materials' characterization and also with another study on a Chinese diatomite used for lead adsorption (Ma et al., 2015). The maximum retention capacities obtained from modelling were 2.8, 4.8, 3.9 and 1.5 mg/g for raw-Da, Da550, Da750 and Da950, respectively.

The highest binding capacity obtained for Da550 is unexpected as two parameters are expected to lead to a diminution of adsorption capacities upon heating treatment. First, as previously discussed, the specific surface slightly decreased (Table 2). Then, it is assumed that nickel and silver ions adsorption onto raw diatomite occurs through the silanol functional groups whose presence has been demonstrated by FTIR. With heating treatment, the silanol sites density declined (Fig. 2) which should lead to a decrease of adsorption capacities. Yet, Da550 presents the highest retention abilities. This could be explained by the higher affinity of Ni towards Al sites rather than Si ones, as previously demonstrated elsewhere (Li et al., 2015; Schulthess and Huang, 1991). As a matter of fact, the Si/Al ratio is sharply decreasing between raw-Da and Da550 (Table SI-1), enhancing Ni retention by Al groups. The Si/Al ratio is the lowest for Da550, which could contribute to its maximal adsorption properties.

As Da550 is the material with the highest retention capacity, it was chosen for all further experiments presented below.

The equilibrium isotherm obtained for silver adsorption by Da550 is presented in Figure 7e. Silver retention was higher to that of nickel (4.4 mg/g). This adsorption isotherm was modeled both by Langmuir and Freundlich models (Figure 8). The equilibrium data (Fig. 7e and Table 5) correlated well with the Freundlich isotherm model with a maximal retention capacity qm estimated at 5.3 mg/g.

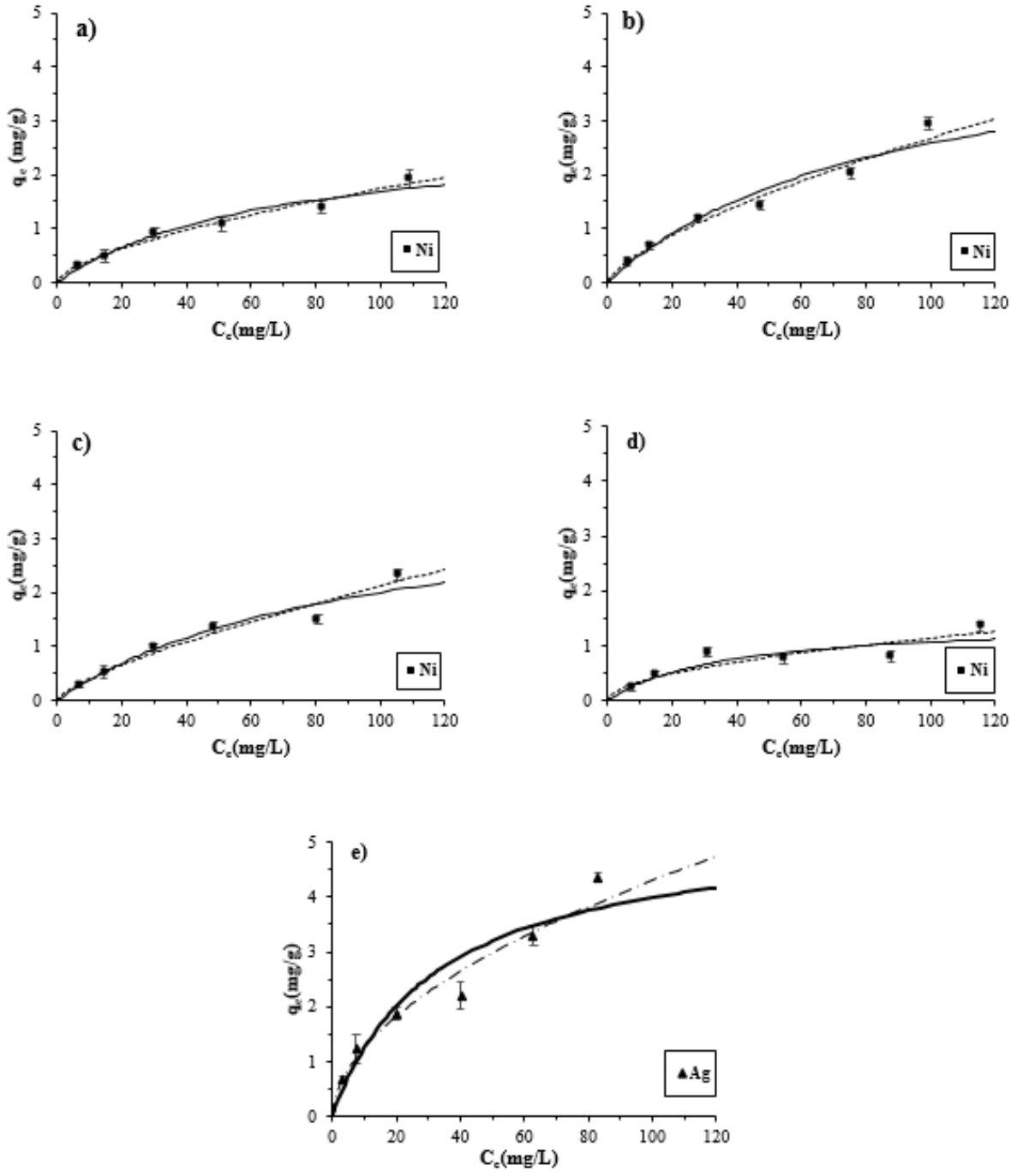

Figure 7. Equilibrium isotherms for nickel adsorption onto raw-Da (a), Da550 (b), Da750 (c) and Da950 (d) and silver adsorption on Da550 (e). The dash and solid lines represent the Freundlich and Langmuir modelling fitting, respectively.

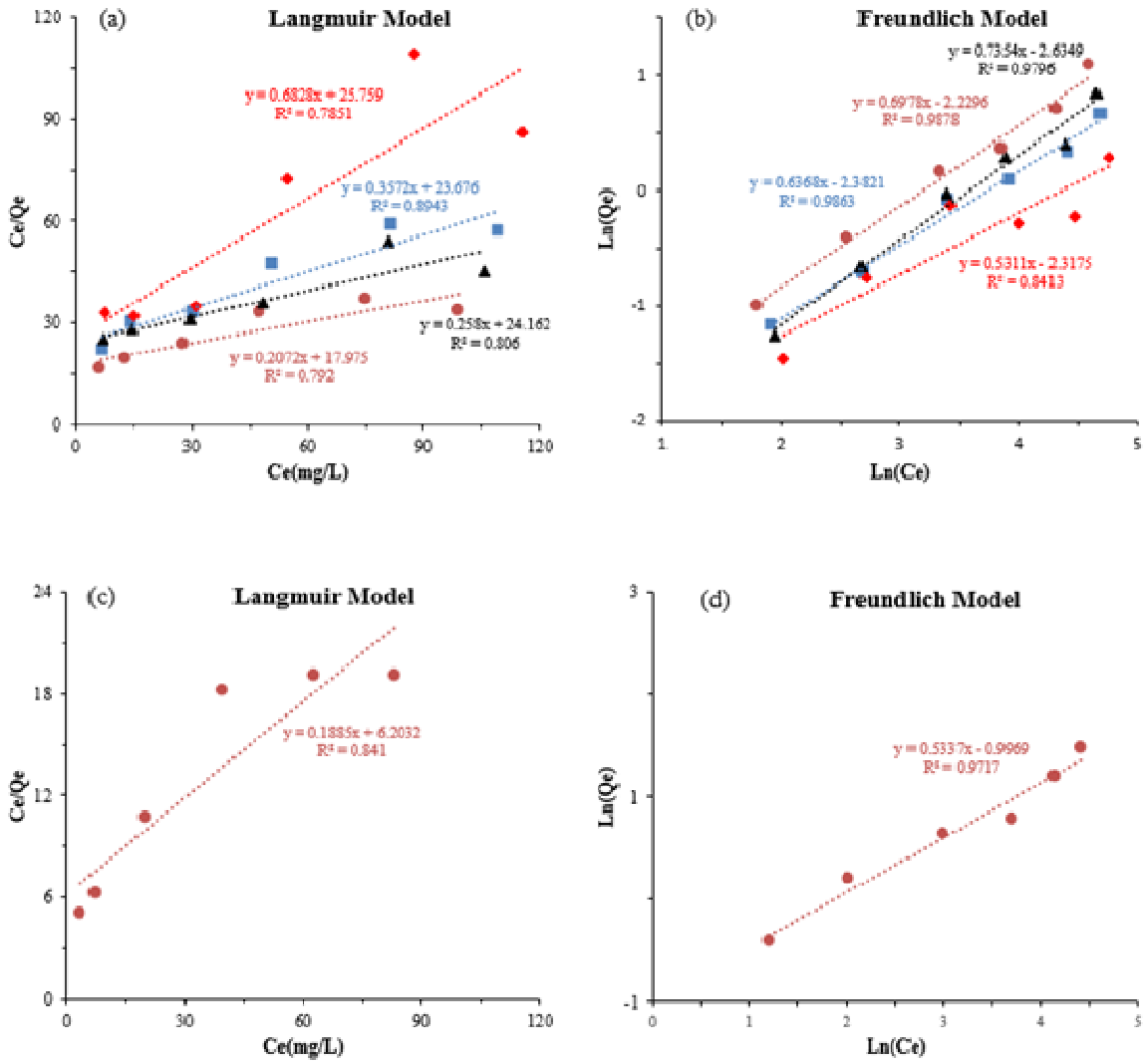

Figure 8. Equilibrium isotherms for nickel adsorption onto raw-Da ( ), Da550 (•), Da750 (Δ) and Da950 (♦) and fitted by Langmuir(a) and Freundlich (b). Silver adsorption on Da550 (•) and fitted by Langmuir (c) and Freundlich (d).

Table 4. Freundlich and Langmuir constants for nickel retention on raw-Da, Da550, Da750 and Da950.

System	**Langmuir model**			**Freundlich model**		
	q_m (mg/g)	K_L (L/mg)	R^2	1/n	K_F (L/mg)	R^2

raw-Da	2.8	0.015	0.894	0.637	0.09	0.986
Da550	4.8	0.011	0.792	0.698	0.11	0.987
Da750	3.9	0.011	0.806	0.735	0.072	0.979
Da950	1.5	0.026	0.785	0.531	0.098	0.841

Table 5. Freundlich and Langmuir constants for silver retention on Da550.

Adsorbent	**Metals Ions**	**System**	**Langmuir model**			**Freundlich model**		
			q_m (mg/g)	K_L (L/mg)	R^2	1/n	K_F (L/mg)	R^2
Da550	Ag	MilliQ-Water	5.3	0.03	0.84	0.534	0.37	0.97

Diatomite studies are scarce and only one focused on nickel retention (ElSayed, 2018). Therefore, the results obtained in this work were compared to the retention capacities of some usual natural adsorbents from the literature (Table 6), chosen for their composition close to that of the studied diatomite. At first, the comparison with the unique other diatomite, Egyptian (ElSayed, 2018), tested for its efficiency towards nickel turned in favor of the diatomite studied in the current work. Yet, it has to be underlined that the experimental conditions were slightly different (nickel concentrations ranging from 0.5 to 10 mg/L at pH 4 in the cited work, compared to 7 in the present work). Looking at the adsorption capacities of the other considered natural materials, Da550 presented a relatively good retention capacity.

Table 6. Comparison of nickel and silver adsorption capacity of natural adsorbents with composition close to that of the studied diatomite.

Metal	Adsorbents	q_m (mg/g)	Reference
Ni	Diatomite (Egypt)	0.23	(ElSayed, 2018)
	Bentonite	2.87	(Vieira et al., 2010)
	ZrO-kaolinite	8.8	(Bhattacharyya and Gupta, 2008)
	Clinoptilolite	1.7	(Argun, 2008)
	K10 montmorillonite clay	2.1	(Carvalho et al., 2008)
	Sepiolite	2.23	(Marmier and Sophia, 2012)
	Raw Da	**1.93**	**Present study**
	Da550	**2.95**	**Present study**
	Da750	**2.3**	**Present study**
	Da950	**1.3**	**Present study**
Ag	Low-rank Turkish Coals	1.87	(Karabakan et al., 2003)
	Expanded perlite	8.46	(Ghassabzadeh et al., 2010)
	Da550	**4.37**	**Present study**

The presence of dissolved organic matter is demonstrated to govern nickel distribution in the environment (Lenoble et al., 2015). The considered dissolved organic matter (humic acid) has a macromolecular structure, with only a small fraction of groups free to interact with metal ions (Sheng et al., 2009). The obtained results (Fig. 9) indicate a significant increase of nickel retention on Da550 with increasing organic matter concentration. This can be partly explained by the complexation of nickel to humic substances (through carboxyl, phenolic and amine functional groups - (Sheng et al., 2009)) followed by the adsorption of these complexes onto Da550, thus enhancing the apparent adsorption. This increased efficiency might also be explained by the fact that humic acid has a strong affinity for mineral surfaces (Ochs et al., 1994; Schlautman and

Morgan, 1994); this affinity undoubtedly modifies the physico-chemical properties at the interface (e.g. charge, pH) that may favor higher retention (Andrew J. Fairhurst , Peter Warwick, 1995).

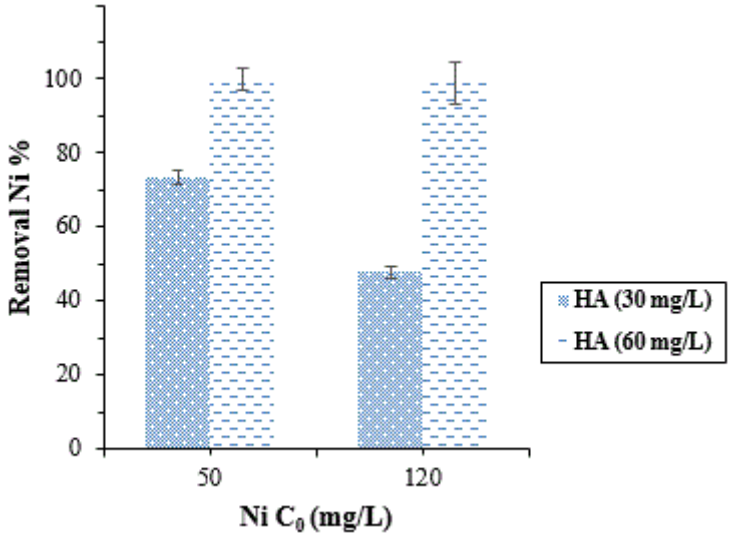

Figure 9. Effect of organic matter (HA) on nickel retention.

3.4. Nickel and silver retention in binary-component systems

The adsorption isotherms of nickel and silver retention by Da550, simultaneously (ratio of 1:1 Ni:Ag) or separately, are shown in Figures 10 and 11. It is apparent that adsorption is higher in the single component systems suggesting competitive effects between nickel and silver ions for adsorption.

The Freundlich and Langmuir parameters are presented in Table 7. The high values of correlation coefficients showed that Freundlich model better fitted the results, in agreement with the results obtained with the single-component systems. The maximum retention capacity in binary-component systems obtained from modelling were 3.8 and 4.2 mg/g for nickel and silver, respectively.

The competitive effects of binary-components can be described by using the ratio of the maximum adsorption capacity for the metal in binary-component system (q_{imix}) to the

maximum adsorption capacity for the same metal in the single-component (q_{im}) (Mohan and Singh, 2002; Zhi-rong and Shao-qi, 2009). If $q_{imix} / q_{im} > 1$, the adsorption is promoted in the presence of the other metal ions; if $q_{imix} / q_{im} = 1$, there is no effect or interaction between metal ion i and other metals ions; if $q_{imix} / q_{im} < 1$, the adsorption is suppressed by the presence of other metal ions. The values of q_{imix}/q_{im} and the rate of equilibrium adsorption reduction (Δ) are shown in Table 7. All values of q_{imix}/q_{im} were less than 1 which confirms the mutual competitive effect of nickel and silver. It should be highlighted that such competition seems usual, whatever the considered metal (Ni/Cu for example, Zhi-rong and Shao-qi, 2009). The rate of equilibrium adsorption reduction (Δ) (eq(6)) of nickel demonstrated a 21.5 % decrease in the binary-component system (Ni-Ag), and for silver, a 21.5 % decrease in the (Ag-Ni) system, which finally demonstrated a common equivalent decrease.

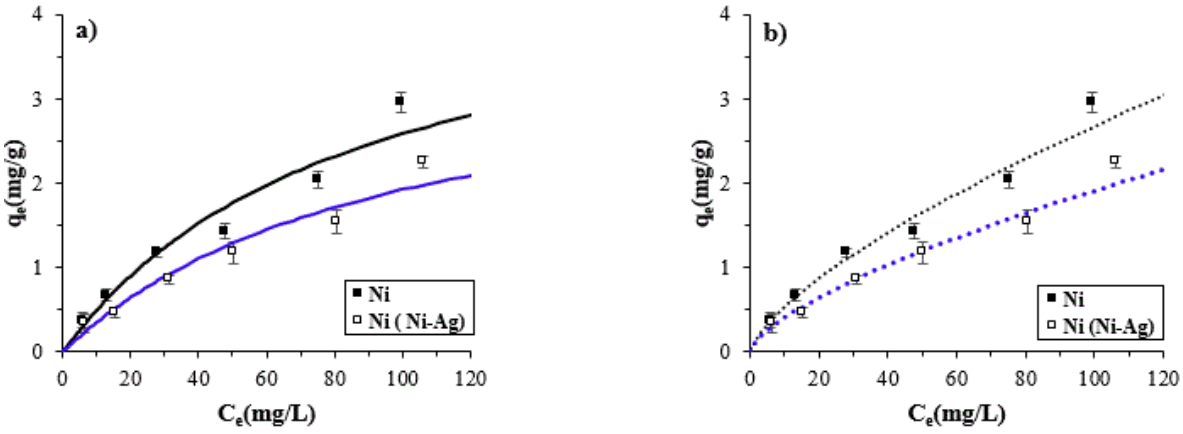

Figure 10. Single and binary nickel adsorption on Da550. The lines represent the fitting by (a) Freundlich and (b) Langmuir modelling.

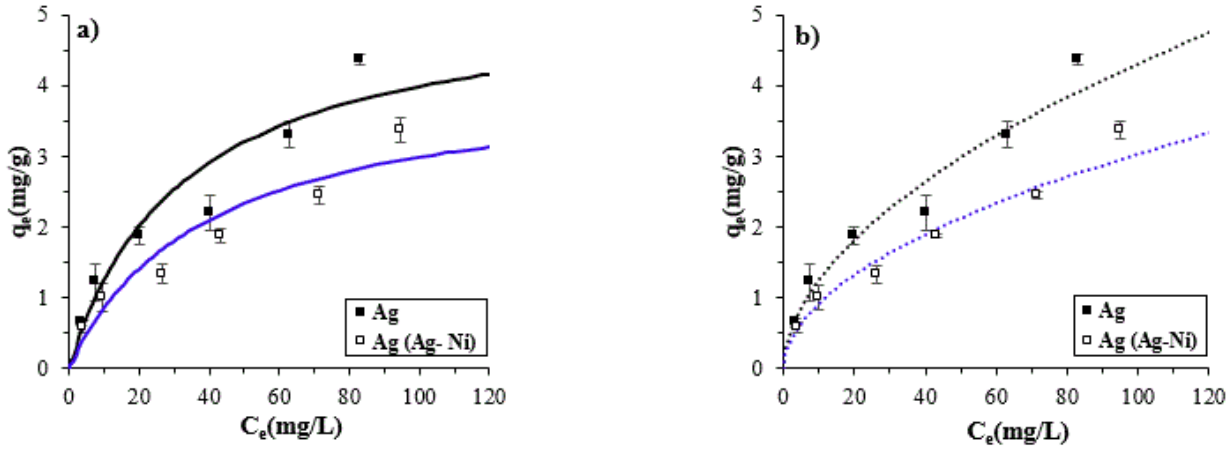

Figure 11. Single and binary silver adsorption on Da550. The lines represent the fitting by (a) Freundlich and (b) Langmuir modelling.

Table 7. Freundlich and Langmuir isotherms constants for single- and binary-component adsorption on Da550

Adsorbent	**Metals Ions**	**Systems**	**Freundlich model**			**Langmuir model**				
			1/n	K_F	R^2	q_{imix}	K_L	R^2	q_{imix}/ q_{im}	Δ (%)
Da550	Ni	Ni-Ag	0.676	0.08	0.979	3.8	0.01	0.758	0.784	21.53
	Ag	Ag-Ni	0.512	0.28	0.975	4.2	0.025	0.845	0.785	21.51

3.5. Nickel and silver retention in real effluents

The brassware effluents (A) are characterized by their really high metal contents. The effluents from Fez (F1) and Sebou rivers (S1) during working days are also polluted in nickel and silver, though to a lesser extent than the brassware effluents. Fez (F2) and Sebou rivers (S2) during non-working day were the least polluted in nickel and silver (Table 1).

The obtained values were compared to environmental quality standards (EQS) concentrations. Nickel and silver concentrations in the studied effluents from Fez and

Sebou rivers during working day (F1 and S1) were above the environmental quality standard (EQS) concentrations of nickel (20µg/L) (EU, 2008) and silver (5µg/L) (Vorkamp and Sanderson, 2016). Nickel and silver concentrations in Fez rivers during non-working day (F2) were also exceeding the environmental quality standard (EQS) concentrations, demonstrating the global low-environmental quality of the ecosystem. Sebou river during non-working day (S2) seemed the only effluent meeting the environmental quality standards of these metals.

In real effluents, the retention of nickel and silver by Da550 might be strongly affected by the presence of many competing agents. We found here that removal of both silver and nickel ions from all our studied effluents were always close to 100% (Figure 12), irrespective of the original concentrations (Table 1). Concerning brassware effluent, Da550 retention capacity was 0.8 mg/g for nickel and 4.1 mg/g for silver. In such complex mixture, a decrease nickel retention capacity was recorded compared to the retained nickel quantity in the single-component systems. Concerning silver, no variation was spotted between the two systems. This result may be due to the presence of ions (chloride for example) in effluents wastewater which could react with silver or lead to precipitation.

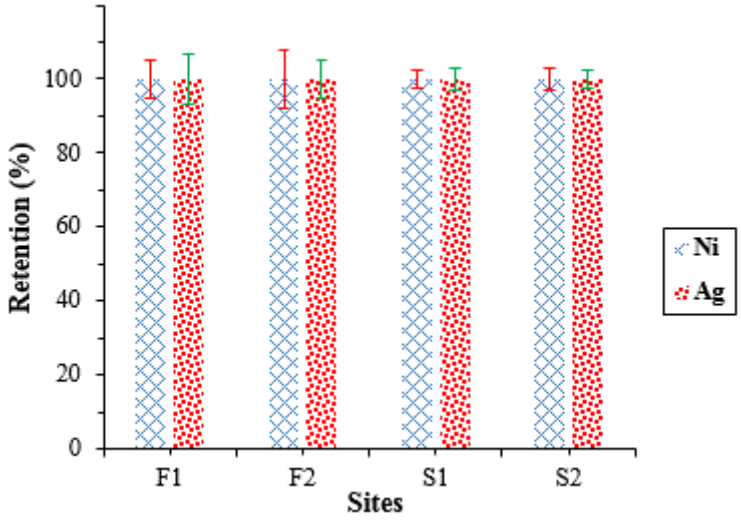

Figure 12. Adsorption of Ni and Ag onto Da550 in Fez and Sebou rivers, sampled during a period of brassware fabrication (F1 and S1) and during a non-working day (F2 and S2).

3.6. Regeneration study

The regeneration and reusability of Da550 adsorbent are very important parameters for a potential industrial application. The impact of regeneration cycles on adsorption capacity is presented in Figure 13. The results showed that for nickel, the adsorbed amount decreased after the first regeneration (2 to 1.6 mg/g) but then remained stable.

For silver, the adsorption capacity decreased by 43%, from 2.9 mg/g to 1.7 mg/g, after five regeneration cycles. In that case, regeneration has a more significant impact on Da550 adsorption capacity. Yet, the remaining retention capacity was still in the upper range when compared to usual natural adsorbent of close composition (Table 6).

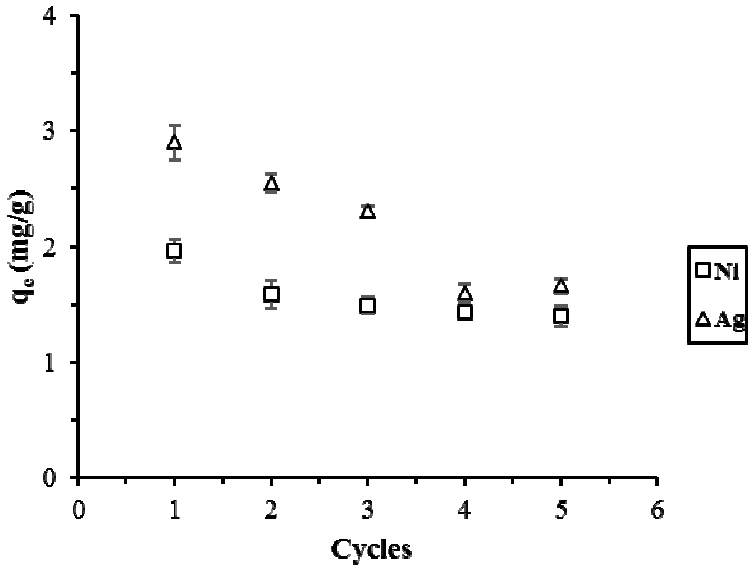

Figure 13. Impact of Da550 regeneration in nickel and silver retention.

4. Conclusions

This paper deals with the use of diatomite for nickel and silver removal from synthetic and real solutions. We found that diatomite calcined to 550 C under air atmosphere was optimum for retention purposes of these 2 metals. The modelling of the obtained results revealed the presence of heterogenous retention sites on the studied material, which indicates the physical adsorption in multilayer on a heterogenous surface. Adsorption parameters agrees favorably with other similar materials reported in the literature. The use of Da550 was then successfully tested in brassware effluent and river effluents, demonstrating the possible use of this worldwide material in wastewaters treatment. Finally, the regeneration of the studied material revealed its extended lifetime. Considering the low cost of Da550, this material should be considered as a viable alternative for the removal of toxic trace metals from waste waters and other natural systems, helping to meet environmental quality standards.

Acknowledgements

The authors wish to thank A. Fahs (Mapiem laboratory, Toulon) for the SEM microscopy and Academy of Finland. The authors are grateful to Pr P. Salaun for his kind and serious checking of our article language.

References

Al-Degs, Y., Khraisheh, M.A.M., Tutunji, M.F., 2001. Sorption of lead ions on diatomite and manganese oxides modified diatomite. Water Research 35, 3724–3728. doi:10.1016/S0043-1354(01)00071-9

Andrew J. Fairhurst , Peter Warwick, S.R., 1995. The influence of humic acid on the adsorption of europium onto inorganic colloids as a function of pH. Engineering 99, 187–199.

Argun, M.E., 2008. Use of clinoptilolite for the removal of nickel ions from water : Kinetics and thermodynamics. Hazardous Materials 150, 587–595. doi:10.1016/j.jhazmat.2007.05.008

Arik, H., 2003. Synthesis of Si3 N4 by the carbo-thermal reduction and nitridation of diatomite. Journal of the European Ceramic Society 23, 2005–2014. doi:10.1016/S0955-2219(03)00038-4

Bahramian, B., Ardejani, F.D., Mirkhani, V., Badii, K., 2010. Diatomite-supported manganese Schiff base: An efficient catalyst for oxidation of hydrocarbons. Applied Catalysis A: General 345, 97–103. doi:10.1016/j.apcata.2008.04.028

Belkhiri, S., Guerza, M., Chouikh, S., Boucheffa, Y., Mekhalif, Z., Delhalle, J., Colella, C., 2012. Textural and structural effects of heat treatment and γ-irradiation on Cs-

exchanged NaX zeolite, bentonite and their mixtures. Microporous and Mesoporous Materials 161, 115–122. doi:10.1016/j.micromeso.2012.05.027

Bhattacharyya, K.G., Gupta, S. Sen, 2008. Adsorption of Fe (III), Co (II) and Ni (II) on ZrO – kaolinite and ZrO – montmorillonite surfaces in aqueous medium. Colloids and Surfaces A: Physicochem. Eng. Aspects 317 317, 71–79. doi:10.1016/j.colsurfa.2007.09.037

Carvalho, W.A., Vignado, C., Fontana, J., 2008. Ni (II) removal from aqueous effluents by silylated clays. Hazardous Materials 153, 1240–1247. doi:10.1016/j.jhazmat.2007.09.083

Cempel, M., Nikel, G., 2006. Nickel : A Review of Its Sources and Environmental Toxicology. polish journal of environmental studies 15, 375–382.

Chaisena, A., Rangsriwatananon, K., 2004. Effects of thermal and acid treatments on some physico-chemical properties of Lampang diatomite. J. Sci. Technol 11, 289–299.

Chang, J., Zhang, J., Tan, B., Wang, Q., Liu, N., Xue, Q., 2020. New insight into the removal of Cd(II) from aqueous solution by diatomite. Environmental Science and Pollution Research. doi:10.1007/s11356-020-07620-y

Dey, S., Podder, S., Roychowdhury, A., Das, D., Kr, C., 2018. Facile synthesis of hierarchical nickel (III) oxide nanostructure : A synergistic remediating action towards water contaminants. Journal of Environmental Management 211, 356–366. doi:10.1016/j.jenvman.2018.01.009

Doumbia, M., Gondo, B., Kwadjo, E., Kouadio, D., Martel, V., Dagnogo, M., 2014. Effectiveness of diatomaceous earth for control of Sitophilus zeamais (Coleoptera : Curculionidae), Tribolium castaneum and Palorus subdepressus (

Coleoptera : Tenebrionidae). Stored Products Research 57, 1–5. doi:10.1016/j.jspr.2013.11.008

El-Sadaawy, M., Abdelwahab, O., 2014. Adsorptive removal of nickel from aqueous solutions by activated carbons from doum seed (Hyphaenethebaica) coat. Alexandria Engineering Journal 53, 399–408. doi:10.1016/j.aej.2014.03.014

ElSayed, E.E., 2018. Natural diatomite as an effective adsorbent for heavy metals in water and wastewater treatment (a batch study). Water Science 32, 32–43. doi:10.1016/j.wsj.2018.02.001

EU, 2008. Directive 2008/105/EC of the European Parliament and of the Council of 16 December 2008 on environmental quality standards in the field of water policy, amending and subsequently repealing Council Directives 82/176/EEC, 83/513/EEC, 84/156/EEC,84/491/EEC,. Official Journal of the European Union L348/84-L348/97. doi:http://eur-lex.europa.eu/legal-content/EN/TXT/?uri=celex:32008L0105

Farhan, A.M., Al-Dujaili, A.H., Awwad, A.M., 2013. Equilibrium and kinetic studies of cadmium(II) and lead(II) ions biosorption onto Ficus carcia leaves. International Journal of Industrial Chemistry 4, 24. doi:10.1186/2228-5547-4-24

Freundlich, H., 1906. Über die Adsorption in Lösungen. Zeitschrift für physikalische Chemie 57, 385–470.

Fu, F., Wang, Q., 2011. Removal of heavy metal ions from wastewaters : A review. Journal of Environmental Management 92, 407–418. doi:10.1016/j.jenvman.2010.11.011

Ghassabzadeh, H., Mohadespour, A., Torab-mostaedi, M., Zaheri, P., Ghannadi, M., Taheri, H., 2010. Adsorption of Ag , Cu and Hg from aqueous solutions using

expanded perlite. Journal of Hazardous Materials 177, 950–955. doi:10.1016/j.jhazmat.2010.01.010

Gu, S., Kang, X., Wang, L., Lichtfouse, E., Wang, C., 2018. Clay mineral adsorbents for heavy metal removal from wastewater: a review. Environmental Chemistry Letters 1–26. doi:10.1007/s10311-018-0813-9

Gunasekaran, T., Nigusse, T., Dhanaraju, M.D., 2012. Silver Nanoparticles as Real Topical Bullets for Wound Healing. JCCW 3, 82–96. doi:10.1016/j.jcws.2012.05.001

Hayzoun, H., Garnier, C., Durrieu, G., Lenoble, V., Bancon-Montigny, C., Ouammou, A., Mounier, S., 2014. Impact of rapid urbanisation and industrialisation on river sediment metal contamination. Environmental Monitoring and Assessment 186, 2851–2865. doi:10.1007/s10661-013-3585-5

Hayzoun, H., Garnier, C., Durrieu, G., Lenoble, V., Poupon, C. Le, Angeletti, B., Ouammou, A., Mounier, S., 2015. Science of the Total Environment Organic carbon , and major and trace element dynamic and fate in a large river subjected to poorly-regulated urban and industrial pressures (Sebou River , Morocco). Science of the Total Environment, The 502, 296–308. doi:10.1016/j.scitotenv.2014.09.014

Inchaurrondo, N., Font, J., Ramos, C.P., Haure, P., 2016. Applied Catalysis B : Environmental Natural diatomites : Efficient green catalyst for Fenton-like oxidation of Orange II. “Applied Catalysis B, Environmental” 181, 481–494. doi:10.1016/j.apcatb.2015.08.022

Karabakan, A., Karabulut, S., Denizli, A., Yürüm, Y., 2003. Removal of Silver (I) from Aqueous Solutions with Low-rank Turkish Coals. Adsorption Science & technology 135–144. doi:10.1260/026361704323150917

Khraisheh, M.A.M., Al-ghouti, M.A., Allen, S.J., Ahmad, M.N., 2005. Effect of OH and silanol groups in the removal of dyes from aqueous solution using diatomite. Water Research 39, 922–932. doi:10.1016/j.watres.2004.12.008

Langmuir, I., 1918. The adsorption of gases on plane surfaces of glass, mica and platinum. Journal of the American Chemical society 345, 1361–1403.

Lenoble, V., Meouche, W., Laatikainen, K., Garnier, C., Brisset, H., Margaillan, A., Branger, C., 2015. Assessment and modelling of Ni(II) retention by an ion-imprinted polymer: Application in natural samples. Journal of Colloid and Interface Science 448, 473–481. doi:10.1016/j.jcis.2015.02.055

Li, C., Zhong, H., Wang, S., Xue, J., Zhang, Z., 2015. A novel conversion process for waste residue: Synthesis of zeolite from electrolytic manganese residue and its application to the removal of heavy metals. Colloids and Surfaces A: Physicochemical and Engineering Aspects 470, 258–267. doi:10.1016/j.colsurfa.2015.02.003

Liang, H., Zhou, S., Chen, Y., Zhou, F., Yan, C., 2015. Diatomite coated with Fe2O3 as an efficient heterogeneous catalyst for degradation of organic pollutant. Journal of the Taiwan Institute of Chemical Engineers 49, 105–112. doi:10.1016/j.jtice.2014.11.002

Liu, H., Zhao, Y., Zhou, Y., Chang, L., Zhang, J., 2019. Removal of gaseous elemental mercury by modified diatomite. Science of the Total Environment 652, 651–659. doi:10.1016/j.scitotenv.2018.10.291

Ma, S.C., Zhang, J.L., Sun, D.H., Liu, G.X., 2015. Surface complexation modeling calculation of Pb(II) adsorption onto the calcined diatomite. Applied Surface Science 359, 48–54. doi:10.1016/j.apsusc.2015.09.133

Marimuthu, S., Antonisamy, A.J., Malayandi, S., Rajendran, K., Tsai, P.C., Pugazhendhi, A., Ponnusamy, V.K., 2020. Silver nanoparticles in dye effluent treatment: A review on synthesis, treatment methods, mechanisms, photocatalytic degradation, toxic effects and mitigation of toxicity. Journal of Photochemistry and Photobiology B: Biology 205, 111823. doi:10.1016/j.jphotobiol.2020.111823

Marmier, N., Sophia, N., 2012. Adsorption of nickel and arsenic from aqueous solution on natural sepiolite S . Ansanay-Alex , C . Lomenech , C . Hurel. International Journal of Nanotechnology 9, 204–215.

Mohamedbakr, H., Burkitbaev, M., 2009. Elaboration and Characterization of Natural Diatomite in Aktyubinsk / Kazakhstan. The Open Mineralogy Journal 3, 12–16. doi:10.2174/1874456700903010012

Mohan, D., Singh, K.P., 2002. Single- and multi-component adsorption of cadmium and zinc using activated carbon derived from bagasse F an agricultural waste $. Water Research 36, 2304–2318.

Nam, S.H., An, Y.J., 2019. Size- and shape-dependent toxicity of silver nanomaterials in green alga Chlorococcum infusionum. Ecotoxicology and Environmental Safety 168, 388–393. doi:10.1016/j.ecoenv.2018.10.082

Nriagu, J., 1988. of worldwide Quantitative assessment contamination of air , water and soils by trace metals. Nature 333, 134–139. doi:10.1038/333134a0

Ochs, M., Ćosović, B., Stumm, W., 1994. Coordinative and hydrophobic interaction of humic substances with hydrophilic Al2O3 and hydrophobic mercury surfaces. Geochimica et Cosmochimica Acta 58, 639–650. doi:10.1016/0016-7037(94)90494-4

Schlautman, M.A., Morgan, J.J., 1994. Adsorption of aquatic humic substances on

colloidal-size aluminum oxide particles: Influence of solution chemistry. Geochimica et Cosmochimica Acta 58, 4293–4303. doi:10.1016/0016-7037(94)90334-4

Schulthess, C.P., Huang, C.P., 1991. Humic and Fulvic Acid Adsorption by Silicon and Aluminum Oxide Surfaces on Clay Minerals. Soil Science Society of America Journal 55, 34–42. doi:10.2136/sssaj1991.03615995005500010006x

Sen, S., Bhattacharyya, K.G., 2008. Immobilization of Pb (II), Cd (II) and Ni (II) ions on kaolinite and montmorillonite surfaces from aqueous medium. Journal of Environmental Management 87, 46–58. doi:10.1016/j.jenvman.2007.01.048

Sheng, G., Wang, S., Hu, J., Lu, Y., Li, J., Dong, Y., Wang, X., 2009. Colloids and Surfaces A : Physicochemical and Engineering Aspects Adsorption of Pb (II) on diatomite as affected via aqueous solution chemistry and temperature. Colloids and Surfaces A: Physicochemical and Engineering Aspects 339, 159–166. doi:10.1016/j.colsurfa.2009.02.016

Stafford, K., Sing, W., Rouquerol, J., 1985. Reporting physisorption data for gas/solid systems with Special Reference to the Determination of Surface Area and Porosity. Pure and Applied.Chemistry 57, 603–619.

Susan E, B., 1999. Review paper a review of potentially low-cost sorbents for heavy metals. Water Research 33, 2469–2472.

Thommes, M., Kaneko, K., Neimark, A. V, Olivier, J.P., Rodriguez-reinoso, F., Rouquerol, J., Sing, K.S.W., 2015. Physisorption of gases , with special reference to the evaluation of surface area and pore size distribution (IUPAC Technical Report). Pure Appl. Chem. doi:10.1515/pac-2014-1117

Uddin, M.K., 2017. A review on the adsorption of heavy metals by clay minerals , with

special focus on the past decade. Chemical Engineering Journal 308, 438–462. doi:10.1016/j.cej.2016.09.029

Vieira, M.G.A., Neto, A.F.A., Gimenes, M.L., Silva, M.G.C., 2010. Sorption kinetics and equilibrium for the removal of nickel ions from aqueous phase on calcined Bofe bentonite clay. Journal of Hazardous Materials 177, 362–371. doi:10.1016/j.jhazmat.2009.12.040

Vorkamp, K., Sanderson, H., 2016. European Environmental Quality Standards (EQS) Variability Study: Analysis of the variability between national EQS values across Europe for selected Water Framework Directive River Basin-Specific Pollutants, Aarhus University, DCE – Danish Centre for Environment and Energy.

Wu, F.C., Tseng, R.L., Huang, S.C., Juang, R.S., 2009. Characteristics of pseudo-second-order kinetic model for liquid-phase adsorption: A mini-review. Chemical Engineering Journal 151, 1–9. doi:10.1016/j.cej.2009.02.024

Zhi-rong, L., Shao-qi, Z., 2009. Adsorption of copper and nickel on Na-bentonite. Process Safety and Environmental Protection 88, 62–66. doi:10.1016/j.psep.2009.09.001

Zhou, Q., Yang, H., Yan, C., Luo, W., Li, X., Zhao, J., 2016. Synthesis of carboxylic acid functionalized diatomite with a micro-villous surface via UV-induced graft polymerization and its adsorption properties for Lanthanum(III) ions. Colloids and Surfaces A: Physicochemical and Engineering Aspects 501, 9–16. doi:10.1016/j.colsurfa.2016.04.030

Table SI-1. Chemical composition of raw and calcined diatomites determined by EDX.

	Wt(%)			
	raw-Da	**Da550**	**Da750**	**Da950**
Na	1.5	1.6	1.1	1.2
Mg	1.2	1.4	1.3	1.3
Al	5.8	7	4.7	4.7
Si	80.6	76.7	82.4	80.1
K	1.9	2.8	2.0	1.7
Ca	3.3	6.6	5.2	7.2
Fe	5.6	3.8	3.2	3.6